

See discussions, stats, and author profiles for this publication at: <https://www.researchgate.net/publication/7100494>

# Mechanism of the Reaction Catalyzed by dl -2-Haloacid Dehalogenase As Determined from Kinetic Isotope Effects †

ARTICLE in BIOCHEMISTRY · JUNE 2006

Impact Factor: 3.02 · DOI: 10.1021/bi0519553 · Source: PubMed

CITATIONS

12

READS

31

9 AUTHORS, INCLUDING:



**Renata Kwiecien**

Lodz University of Technology

14 PUBLICATIONS 184 CITATIONS

SEE PROFILE



**Rafal Kaminski**

Lodz University of Technology

29 PUBLICATIONS 176 CITATIONS

SEE PROFILE



**Lukasz Szatkowski**

The University of Arizona

14 PUBLICATIONS 59 CITATIONS

SEE PROFILE



**Piotr Paneth**

Lodz University of Technology

173 PUBLICATIONS 1,974 CITATIONS

SEE PROFILE

## Mechanism of the Reaction Catalyzed by DL-2-Haloacid Dehalogenase As Determined from Kinetic Isotope Effects<sup>†</sup>

Ewa Papajak,<sup>‡</sup> Renata A. Kwiecień,<sup>‡</sup> Juliusz Rudziński,<sup>‡</sup> Daria Sicińska,<sup>‡</sup> Rafał Kamiński,<sup>‡</sup> Łukasz Szatkowski,<sup>‡</sup> Tatsuo Kurihara,<sup>§</sup> Nobuyoshi Esaki,<sup>§</sup> and Piotr Paneth<sup>\*‡</sup>

*Institute of Radiation Chemistry, Department of Chemistry, Technical University of Lodz, Żeromskiego 116, 90-924 Lodz, Poland, and Laboratory of Molecular Microbial Science, Institute for Chemical Research, Kyoto University, Uji, Kyoto 611-0011, Japan*

*Received September 27, 2005; Revised Manuscript Received March 21, 2006*

**ABSTRACT:** DL-2-Haloacid dehalogenase from *Pseudomonas* sp. 113 is a unique enzyme because it acts on the chiral carbons of both enantiomers, although its amino acid sequence is similar only to that of D-2-haloacid dehalogenase from *Pseudomonas putida* AJ1 that specifically acts on (R)-(+)-2-haloalkanoic acids. Furthermore, the catalyzed dehalogenation proceeds without formation of an ester intermediate; instead, a water molecule directly attacks the  $\alpha$ -carbon of the 2-haloalkanoic acid. We have studied solvent deuterium and chlorine kinetic isotope effects for both stereoisomeric reactants. We have found that chlorine kinetic isotope effects are different:  $1.0105 \pm 0.0001$  for (S)-(–)-2-chloropropionate and  $1.0082 \pm 0.0005$  for the (R)-(+)-isomer. Together with solvent deuterium isotope effects on  $V_{\max}/K_M$ ,  $0.78 \pm 0.09$  for (S)-(–)-2-chloropropionate and  $0.90 \pm 0.13$  for the (R)-(+)-isomer, these values indicate that in the case of the (R)-(+)-reactant another step preceding the dehalogenation is partly rate-limiting. Under the  $V_{\max}$  conditions, the corresponding solvent deuterium isotope effects are  $1.48 \pm 0.10$  and  $0.87 \pm 0.27$ , respectively. These results indicate that the overall reaction rates are controlled by different steps in the catalysis of (S)-(–)- and (R)-(+)-reactants.

DL-2-Haloacid dehalogenase from *Pseudomonas* sp. 113 (DL-DEX 113) catalyzes the hydrolytic dehalogenation of both D- and L-2-haloalkanoic acids (1). The gene encoding DL-DEX 113 has been isolated and sequenced (1). The open reading frame consists of 921 bp corresponding to 307 amino acid residues. The protein molecular mass was estimated to be 34.2 kDa. Twenty-six residues of DL-DEX 113 that are conserved between DL-DEX 113 and D-2-haloacid dehalogenase were subjected to site-directed mutagenesis (2). From these studies, Thr65, Glu69, and Asp194 were found to be essential for the dehalogenation of both (R)-(+)-2-haloalkanoic acids and (S)-(–)-2-haloalkanoic acids. The activities of each of the 26 mutant enzymes toward (R)-(+)- and (S)-(–)-2-chloropropionate were almost equal. Moreover, (R)-(+)-2-chloropropionate competitively inhibits the enzymatic dehalogenation of (S)-(–)-2-chloropropionate, and vice versa. On the basis of these results, it is proposed that both enantiomers share a common active site of DL-DEX 113.

Two properties of this enzyme make it unique. First, it acts on the chiral carbons of both enantiomers, although the amino acid sequence of DL-DEX 113 is similar only to that of D-2-haloacid dehalogenase from *Pseudomonas putida* AJ1 that specifically acts on (R)-(+)-2-haloalkanoic acids (3). Some of the residues (23.5%) are completely conserved

between these two enzymes, while there is no sequence similarity between DL-DEX 113 and L-2-haloacid dehalogenases. Second, other dehalogenases studied previously have an active site carboxylate group that attacks the substrate carbon atom bound to the halogen atom, leading to the formation of an ester intermediate, which is subsequently hydrolyzed (Figure 1A). The reaction catalyzed by DL-DEX 113, on the other hand, proceeds without formation of an ester intermediate. <sup>18</sup>O tracer studies (4, 5) indicated that solvent directly attacks the  $\alpha$ -carbon of 2-haloalkanoic acid to displace the halogen atom (Figure 1B).

We have shown that chlorine kinetic isotope effects (KIEs) can provide valuable insight into mechanisms of various dehalogenases (6, 7). Herein, we present the results of chlorine KIEs on the dehalogenation of both stereoisomers of 2-chloropropionate, which enabled us to shed new light on the mechanism of DL-DEX 113.

### MATERIALS AND METHODS

**Enzyme and Chemicals.** DL-DEX 113 was purified from recombinant *Escherichia coli* JM109 harboring p4b-1, constructed for overproduction of the enzyme as described previously (2). The cells were grown at 37 °C in Luria-Bertani medium containing 100  $\mu$ g/mL ampicillin. When the OD<sub>600</sub> reached 3.0, IPTG (final concentration of 0.2 mM) was added, and cultivation was continued for 3 h. The cells were harvested by centrifugation, rinsed twice with 50 mM potassium phosphate buffer (pH 7.0), and stored at –80 °C. The cells collected from the 1 L culture were suspended with 40 mL of 50 mM potassium phosphate buffer (pH 7.0) and

<sup>†</sup> This work was supported by Grant 4/T09A/030/25 (2003–2006) from the State Committee for Scientific Research (KBN, Poland).

<sup>\*</sup> To whom correspondence should be addressed. Telephone: (+4842) 631-3199. Fax: (+4842) 636-5008. E-mail: paneth@p.lodz.pl.

<sup>‡</sup> Technical University of Lodz.

<sup>§</sup> Kyoto University.

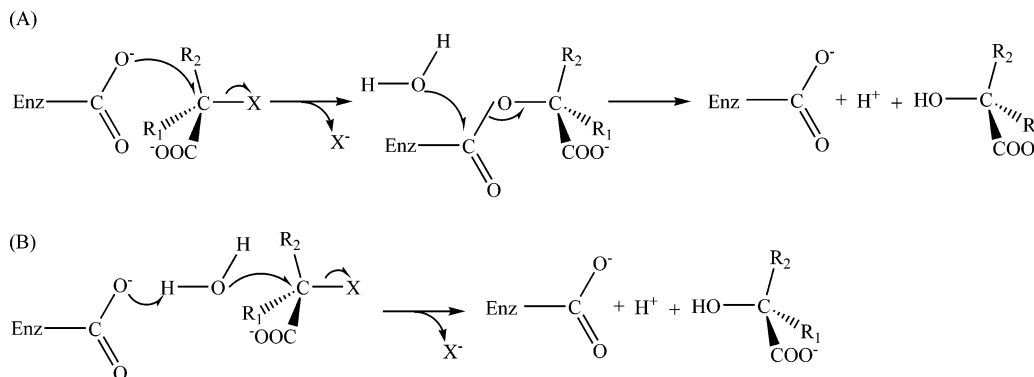


FIGURE 1: (A) Two-step dehalogenation involving formation of the enzyme intermediate usually encountered in bacterial dehalogenases. (B) Proposed mechanism of dehalogenation catalyzed by DL-DEX 113.

disrupted by sonication. The soluble fraction was obtained after centrifugation at 4500g for 20 min. Ammonium sulfate was added to the soluble fraction to 40% saturation, and the precipitate was removed by centrifugation at 4500g for 30 min. The supernatant solution was applied to a Butyl Toyopearl 650M column (TOSOH, Tokyo, Japan), and elution was carried out with a linear gradient from 30 to 0% saturation of ammonium sulfate in 50 mM potassium phosphate buffer (pH 7.0). The enzyme activity was measured by determination of the amount of chloride ions released from (*R*)-(+)- or (*S*)-(–)-2-chloropropionic acid as described previously (2). The active fraction was pooled, dialyzed against 50 mM potassium phosphate buffer (pH 7.0), and concentrated by ultrafiltration. The preparation was shown to be homogeneous by SDS–polyacrylamide gel electrophoresis. The specific activity of the enzyme is 42 units/mg.

(*R*)-(+)-2-Chloropropionic acid and (*S*)-(–)-2-chloropropionic acid (>99% pure, Fluka) were used as the substrates. Bis-tris-propane was obtained from CalBiochem and from Fluka. Mercuric(II) thiocyanate (pure for analysis, pure p.a.) was purchased from Fluka and ferric ammonium sulfate from LPP-H “OCh” (Lublin, Poland). Nitric acid (pure p.a.), NaOH (pure p.a.), silver nitrite (pure p.a.), NaHCO<sub>3</sub> (pure p.a.), KH<sub>2</sub>PO<sub>4</sub> (pure p.a.), and Na<sub>2</sub>HPO<sub>4</sub> (pure p.a.) were supplied by POCh (Gliwice, Poland). Concentrated sulfuric acid (suprapure) was obtained from Merck. These materials were used without further purification. Water was purified by the Nanopure II system (Barnstead). D<sub>2</sub>O (>99.8%) was obtained from Armar Chemical.

**Kinetic Assays.** For chloride kinetic isotope effect measurements, the 2-chloropropionic acid (final concentration of 20 mM) was dissolved in 100 mL of chloride ion-free 100 mM bis-tris-propane buffer and the pH of the solution was brought to 9.5 by addition of nitric acid and controlled using an MA235 pH/ion analyzer (Mettler Toledo). The mixture was thermostated at 37 °C, and then the reaction was initiated by addition of 7.25 units (100 μL) of DL-DEX 113. The progress of the reaction was determined by monitoring chloride concentration using a spectrophotometric assay. The absorption spectra were recorded using a PC-controlled PU 8710 (Philips) or Cary 300 Conc (Varian) UV–vis spectrophotometer in a 1 cm cuvette semi-micro high form, with two clear sides (Kartell) with a resolution of 0.1 nm. The method was based on colorimetric measurement of the iron(III) thiocyanate complex which resulted from reaction of chloride with mercuric(II) thiocyanate to

give HgCl<sub>2</sub> and thiocyanate, which then combined with Fe-(III) (8). The procedure was adjusted to our conditions and concentration range. At appropriate times, predefined on the basis of calibration of the procedure with known amounts of reactant, 50.0 μL aliquots of the reaction mixture were taken and injected into 80 μL of a 0.25 M solution of iron-(III) ammonium sulfate in an 8.5 M nitric acid solution with 80 μL of a saturated solution of mercuric(II) thiocyanate in ethanol. The mixture was shaken and diluted with 840 μL of H<sub>2</sub>O in a cuvette and mixed again. Exactly after 4 min, the absorbance was measured in a spectrophotometer against water at 460 nm.

At the required fraction of conversion, reaction mixtures were quenched by addition of concentrated nitric acid until the final solution pH reached 1–2 and chloride was precipitated with silver nitrate. The precipitate was centrifuged for 3 min at 5000g, washed with 20 mL of water, and centrifuged again. The washing procedure was repeated three times, and AgCl was left to dry in a desiccator in the dark; it was subsequently used for the isotopic analysis of chloride. For chlorine isotopic analysis of the reactant, samples (~10 mg) were placed in combustion tubes filled with hydrogen peroxide and combusted. Combustion products were eluted with a 30% aqueous ethanol solution. AgCl was precipitated with silver nitrite and purified by the procedure described above.

For solvent kinetic isotope effect measurements, to 4 mL of a solution of 2-chloropropionic acid with an initial concentration in the range of 0.8–24 mM with a buffer concentration of 50 mM [pH (pD) 9.5] and a temperature of 37 °C, 10 μL of the enzyme solution was added (see above). A standard correction for the pD reading of the standard glass electrode was added (9). At the required time intervals (1–3 min), reactions were quenched by addition of 0.4 mL of iron ammonium sulfate in nitric acid. The spectrophotometric determination of concentrations was performed as described above.

**Chlorine Isotopic Analysis and KIEs.** The isotopic ratios ( $R = I_{37}/I_{35}$ ) were measured by the FAB-IRMS (fast atom bombardment isotope ratio mass spectroscopy) technique developed in our laboratory as described previously (10) using a modified, hybrid model MI 1201E mass spectrometer (PO Electron). Samples (~5 mg) of silver chloride (per measurement) were placed on the tip of clean silver plates that had been washed with nitric acid, water, and acetone, and the plates were heated gently to melt the sample. Precautions not to exceed 480 °C and to keep the dimensions

Table 1: Experimental Values of the Chlorine KIEs for (*R*)-(+)- and (*S*)-(–)-2-Chloropropionates

<i>f</i>	$(I_{37}/I_{35})_{S(-)}$	$(k_{35}/k_{37})_{S(-)}$	$(I_{37}/I_{35})_{R(+)}$	$(k_{35}/k_{37})_{R(+)}$
0	0.32237 <sup>a</sup>		0.32215 <sup>a</sup>	
0.164			0.31980	1.0080
0.145			0.31953	1.0089
0.122			0.31981	1.0079
0.138			0.31972	1.0082
0.156	0.31927	1.0106		
0.197	0.31933	1.0106		
0.17	0.31936	1.0104		
0.175	0.31935	1.0104		
mean		1.0105 ± 0.0001 <sup>b</sup>		1.0082 ± 0.0005 <sup>b</sup>

<sup>a</sup> Average of three separate measurements. <sup>b</sup> Standard deviation.Table 2: Summary of the Solvent Deuterium Kinetic Isotope Effects<sup>a</sup>

	<i>S</i>	<i>R</i>
$V_{\max}$	1.48 ± 0.10	0.87 ± 0.27
$V_{\max}/K_M$	0.78 ± 0.09	0.90 ± 0.13

<sup>a</sup> Standard deviations are reported.

of the samples constant (~0.2 mm thick and 4 mm in diameter) were taken. The silver plate with the adherent solid sample was mounted on the tip of the direct insertion probe. Xenon atoms of 6 keV hitting the surface of the probe at an incidence angle of 45° were used for ionization. The negative ions formed in this way were accelerated through a 5 kV potential and detected in the Faraday cup collector system. The spectra contained almost exclusively chloride peaks at  $m/z$  35 and 37.

The observed chlorine isotope effects were calculated from the equation

$$k_{35}/k_{37} = \ln(1 - f)/\ln(1 - fR_f/R_0) \quad (1)$$

where  $k_{35}/k_{37}$  is the chlorine kinetic isotope effect,  $f$  is the fraction of the reaction, and  $R_i$  values are isotopic ratios of the product after the fraction of reaction  $f$  ( $R_f$ ) and of the reactant before the reaction is started ( $R_0$ ).

**Solvent KIEs.** Solvent kinetic isotope effects were obtained from the nonlinear regression analysis of eq 2, which describes Michaelis–Menten kinetics with statistical estimators being directly  $V_{\max}/K_M$  and  $V_{\max}$ :

$$v = \frac{[S]}{\frac{1}{V_{\max}/K_M} + \frac{[S]}{V_{\max}}} \quad (2)$$

where  $v$  is the initial rate and  $[S]$  the reactant concentration. Table 2 lists values obtained at pL 9.5 and 37 °C. Experiments in light and heavy solvent in the pL range of 8–10 confirmed that these results are obtained around the maximum on the pL profile (data not shown).

**Chlorine KIE Calculations.** Structures of reactants and the transition state were obtained at the DFT level using the MPW1K (11) theory level in the LACV3P\*\* basis set (12) and the Poisson–Boltzmann (PB) solvation model (13) as implemented in Jaguar (12). After optimization, the isotopic vibrational analysis was performed and transition states were identified by one imaginary frequency, corresponding to a transition from reactants to products (having only real

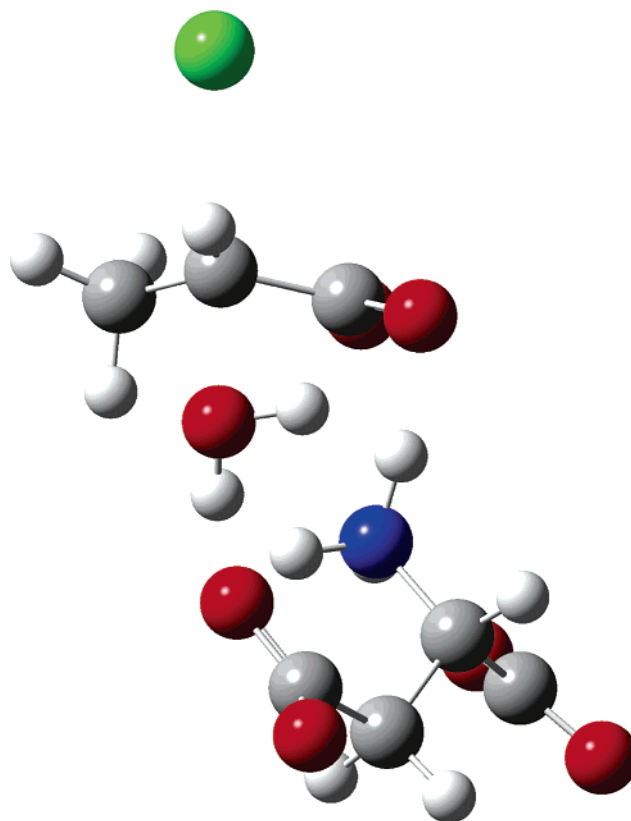


FIGURE 2: Models of the transition state in the active site.

harmonic vibrational frequencies). The structure of 2-chloropropionate was optimized using water parameters. In lieu of the three-dimensional structure of DL-DEX 113, the model of the transition state in the active site included 2-chloropropionate, an attacking water molecule, and an aspartate residue that was placed within hydrogen bonding distance behind the water molecule acting as the general base proton acceptor (Figure 2). Solvent parameters for THF, which is considered a reasonable model for the active sites of enzymes, have been used (14).

Intrinsic chlorine KIEs were calculated from the Bigeleisen equation (15) using ISOEFF98 (16):

$$\frac{k_{35}}{k_{37}} = \frac{\nu_{35}^{3n-6} \prod_i \frac{\sinh(u_{i37}/2)}{u_{i37}}}{\nu_{37}^{3n-6} \prod_i \frac{\sinh(u_{i35}/2)}{u_{i35}}} \frac{\sinh(u_{i37}^{\neq}/2)}{u_{i37}^{\neq}} \frac{\sinh(u_{i35}^{\neq}/2)}{u_{i35}^{\neq}} \quad (3)$$

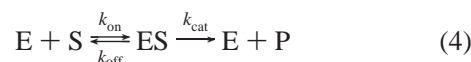
where  $u = hv/k_B T$  ( $h$  and  $k_B$  are Planck's and Boltzmann's constants, respectively and  $T$  is the absolute temperature),  $n$  is the number of atoms, and  $\nu_i$  values are the frequencies of normal modes of vibrations. A superscript  $\neq$  indicates the properties of the transition state, and subscripts 35 and 37 identify the isotopic species. One-dimensional Wigner correction for tunneling (17) has been included as suggested recently also for heavy-atom isotope effects (18). It turned out to be negligible (<1.0002) in reactions studied here.

## RESULTS AND DISCUSSION

Although DL-DEX 113 catalyzes the hydrolysis of both stereoisomers of 2-chloropropionic acid, the corresponding chlorine kinetic isotope effects (KIEs) are different. For (*S*)-(–)-2-chloropropionate, we have found (Table 1) a very large



isotope effect of  $1.0105 \pm 0.0001$ . This value is at the edge of the range for chlorine KIEs on dehalogenations (19) and in fact is the largest measured in enzymatic systems so far (20). The isotope effect found for the (*R*)-(+)-isomer is, on the other hand, considerably smaller and equal to  $1.0082 \pm 0.0005$ . Since there is kinetic evidence that both stereoisomers bind to the same active site, the question arises of why these isotope effects are different. There are two possible explanations which are discussed below on the basis of the simplest kinetic model:



where E, S, and P are the enzyme, reactant, and product, respectively, and  $k_i$  ( $i = \text{on, off, or cat}$ ) values are individual rate constants of the reactant association with and dissociation from the enzyme and forward reaction of the Michaelis complex, respectively. The observed kinetic isotope effect is related to the so-called intrinsic isotope effect (here the isotope effect on the rate constant  $k_{\text{cat}}$ ) by the equation

$$^{37}(V_{\text{max}}/K_M)_{\text{obs}} = \frac{^{37}k_{\text{cat}} + k_{\text{cat}}/k_{\text{off}}}{1 + k_{\text{cat}}/k_{\text{off}}} \quad (5)$$

in which chlorine KIEs ( $k_{35}/k_{37}$ ) are denoted by  $^{37}k$ , for brevity using the Northrop notation (21). The  $k_{\text{cat}}/k_{\text{off}}$  ratio is called forward commitment to catalysis (or commitment for short). The assumption used in the derivation of eq 5 is that the binding step does not contribute to the isotopic fractionation, which is reasonable in the case of chlorine KIEs (22).

Inspection of eq 5 indicates that two scenarios lead to different chlorine KIEs for the stereoisomers. In the limiting case, when the commitment approaches zero the observed KIE approaches the value of the intrinsic KIE. If this were the case for DL-DEX 113, it would mean that the intrinsic KIEs for the enantiomers are different and equal to the experimentally observed KIEs. At the other extreme, the intrinsic chlorine KIEs for both enantiomers could be equal and the difference in the observed KIEs results from different commitments.

DL-DEX 113 is homologous with D-2-haloacid dehalogenase and not homologous with enzymes that use the (*S*)-(–)-enantiomer. It is thus possible that one of the enantiomers is oriented in the active site pocket differently than the other, and therefore some interactions with the protein residues that influence the magnitude of the intrinsic KIE may be different for the two enantiomers. However, the alternative explanation that the larger of the chlorine KIEs is practically equal to the intrinsic value and the other is smaller due to a commitment cannot be ruled out. To differentiate between these two mechanisms, we have measured solvent deuterium isotope effects for reactions of both stereoisomers.

Solvent isotope effects, collected in Table 2, were obtained by direct fitting of the experimental results to eq 2. Available methods that can be used to assay the progress of dehalogenation suffer from the fact that they cannot be used in the continuous way. The obtained solvent isotope effects carry, therefore, significant statistical uncertainty. In such cases, the proper statistical treatment becomes an important issue. Since we are interested in isotope effects on  $V_{\text{max}}/K_M$  and  $V_{\text{max}}$ , these two quantities (rather than  $V_{\text{max}}$  and  $K_M$  used in

the Michaelis–Menten equation in its typical form) were treated as statistical estimators. As can be seen, the solvent isotope effect on  $V_{\text{max}}/K_M$  for the (*R*)-(+)-stereoisomer is slightly smaller (closer to unity) than the one obtained for the (*S*)-(–)-substrate. This parallels the relationship between chlorine KIEs for these two substrates. Together, these observations suggest the presence of a step that precedes the dehalogenation step and is partly rate-limiting under  $V_{\text{max}}/K_M$  conditions in the case of the (*R*)-(+)-substrate.

Generally, fractionation factors for the transition states of proton transfer reactions are significantly inverse, leading to normal solvent KIEs. Thus, at the first glance reported here, solvent isotope effects on  $V_{\text{max}}/K_M$  are somewhat puzzling. Inverse solvent isotope effects on  $V_{\text{max}}/K_M$  can be associated with the direct nucleophilic attack of the hydroxide ion (23), which is, however, not the case in the DL-DEX 113 reaction. Another explanation of the inverse  $^D V_{\text{max}}/K_M$  seems to be the assumption that in the transition state the proton from the attacking water molecule is practically fully transferred to the general base and the fractionation factors from the transition state are overbalanced by the fractionation from substrates. This explanation, however, requires the fractionation factor of the reactant to be significantly inverse. A reasonable candidate for the role of general base would be a cysteine. However, DL-DEX 113 has only one cysteine residue at position 177 that is not conserved among DL-DEX enzymes from various species; e.g., DL-DEX from *Methylobacterium* sp. CPA1 has no cysteine at all. Furthermore, the enzyme is not inactivated by the treatment of various cysteine-modifying reagents such as *p*-chloromercuribenzoic acid and iodoacetamide. These observations suggest that it is very unlikely that cysteine plays a catalytically important role in DL-DEX 113. An inverse solvent KIE may originate in binding. Thus, an alternative explanation of the observed isotopic pattern of chlorine and hydrogen is that the dehalogenation step is preceded by a kinetically coupled process that is sensitive to deuterium substitution. This interpretation has been offered by Stein and Trainor (24), who found a pattern of solvent KIEs [ $^D V_{\text{max}} = 1.58 \pm 0.07$  and  $^D(V_{\text{max}}/K_M) = 0.65 \pm 0.05$ ] for elastase inhibition that leads to dehalogenation, which is essentially the same as the one found in this work for the (*S*)-(–)-isomer. The exact nature of the noncovalent binding process that can lead to inverse solvent isotope effects remains obscured and controversial (9).

To investigate the origin of the isotopic fractionations, we have modeled overall and intrinsic KIEs. Our previous site-directed mutagenesis studies suggest that the water molecule, which acts as the nucleophile, is activated by an aspartate or glutamate that also is the acceptor of the proton. Thus, we have built models of the ES complex and the transition state for the dehalogenation step that included an aspartate residue, a water molecule, and the substrate. The reduced polarity of the enzyme active site was mimicked by using the continuum solvent model with the dielectric constant of 7.5. The calculations were performed at the DFT level using the MPW1K functional. In our previous theoretical studies (25, 26) on a simple  $S_N2$  reaction, in which the chlorine is being displaced, we have shown that DFT methods give values of the chlorine KIE closest to the experiment. The structure of the optimized transition state is illustrated in Figure 2, and its major geometrical features are listed in

Table 3: Properties of the Transition State and Isotope Effects in Dehalogenations Catalyzed by DL-DEX 113 Obtained at the PB/MPW1K/LACV3P\*\* Level

property	value	property	value
$R(\text{C}-\text{Cl})$ (Å)	2.53	$\nu_L^\infty$ (cm <sup>-1</sup> )	424.0i
$R(\text{O}-\text{C})$ (Å)	2.05	$^{37}k_{\text{cat}}$	1.0089
$R(\text{O}-\text{H})$ (Å)	0.99	$^{37}(V_{\text{max}}/K_M)$	1.0100
$R(\text{H}\cdots\text{O})$ (Å)	1.63	$^Dk_{\text{cat}}$	1.16
$\angle\text{O}-\text{H}\cdots\text{O}$ (deg)	167.2	$^D(V_{\text{max}}/K_M)$	0.76
$\angle\text{Cl}-\text{C}-\text{O}$ (deg)	156.6		

Table 3. As can be seen, the proton in the flight is still on the water molecule in the transition state, although the O–H bond is elongated by  $\sim 0.03$  Å from its equilibrium distance. The values for the intrinsic KIEs were obtained from ES and transition state harmonic vibrations. Theoretical values for the isotope effects under  $V/K$  conditions were obtained using the same transition state structure and reactants (water molecule and 2-chloropropionate) in aqueous solution modeled using the PB continuum solvent model with parameters for water. The agreement of both overall chlorine and solvent deuterium KIEs obtained on the basis of this model with values obtained experimentally for the (S)-(–)-isomer is very good. It should be noted that the inverse value of the solvent deuterium KIE comes from a step that precedes dehalogenation, which supports the conclusions of Stein and Trainor and indicates that such an inverse value may originate from isotopic fractionation of a single water molecule upon its transfer from bulk solution to the nonpolar active site of the enzyme.

The isotopic data collected in this work allow us to gain some more information about the mechanism. The equation analogous to eq 5 for the deuterium isotope effects is given by

$$^D(V_{\text{max}}/K_M)_{\text{obs}} = ^Dk_{\text{on}} \frac{^Dk_{\text{cat}}/^Dk_{\text{off}} + k_{\text{cat}}/k_{\text{off}}}{1 + k_{\text{cat}}/k_{\text{off}}} \quad (6)$$

and includes kinetic isotope effects on all individual rate constants. Assuming that the observed chlorine KIE for the (S)-(–)-isomer is practically equal to the intrinsic chlorine KIE from the observed value for the (R)-(+)-isomer, we can evaluate the value of the commitment  $k_{\text{cat}}/k_{\text{off}}$  to be equal to  $\sim 0.28$ . Using this value together with the calculated intrinsic  $^Dk_{\text{cat}}$  from Table 3 and the observed value of the solvent KIE for the (R)-(+)-isomer, we can rewrite eq 6 to the form

$$0.9 = ^Dk_{\text{on}} \frac{1.16/^Dk_{\text{off}} + 0.28}{1.28} \quad (7)$$

Additionally, the relation between  $^Dk_{\text{on}}$  and  $^Dk_{\text{off}}$  can be evaluated from both experimental ( $^DV_{\text{max}}/K_M$  and  $^DV_{\text{max}}$ ) and theoretical ( $^DV_{\text{max}}/K_M$  and  $^Dk_{\text{cat}}$ ) values of deuterium isotope effects for the (S)-(–)-isomer. The corresponding values are 0.53 and 0.66, respectively. Using the mean value of 0.59, we can solve for isotope effects on all individual rate constants. The resulting values are 1.67 for  $^Dk_{\text{on}}$  and 2.83 for  $^Dk_{\text{off}}$ . Although these numbers are not very precise due to the accumulation of statistical errors, they shed some light on the source of the inverse solvent deuterium isotope effect.

Interpretation of solvent isotope effects in the  $V_{\text{max}}$  regime is much simpler. For the (S)-(–)-substrate, the solvent KIE

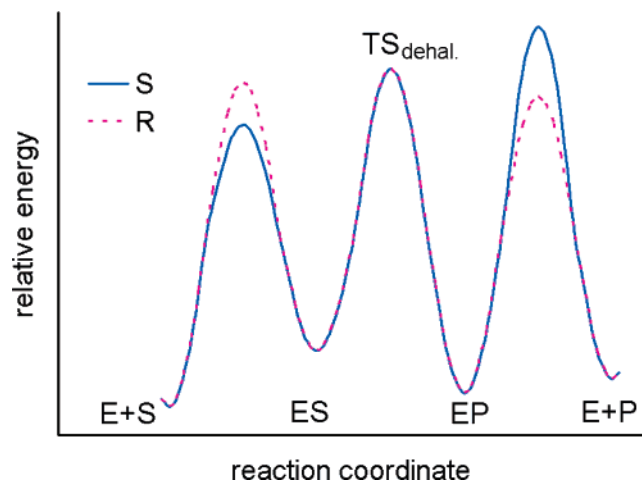


FIGURE 3: Energy profiles for reactions of 2-chloropropionate enantiomers catalyzed by DL-DEX 113.

on  $V_{\text{max}}$  is much larger than that on  $V_{\text{max}}/K_M$ , indicating that the overall rate-limiting step is shifted from the dehalogenation to a step that follows it. In the case of the other stereoisomer, solvent KIEs on these two kinetic parameters are equal, suggesting that the dehalogenation is both the first irreversible and rate-determining step in the overall catalysis.

On the basis of experimental values of chlorine and solvent deuterium KIEs for both enantiomers of 2-chloropropionate, several conclusions can be drawn.

Very large experimental values of chlorine KIEs together with DFT results support our previous finding that dehalogenation proceeds via a direct nucleophilic attack of an enzyme-activated water molecule.

Values of experimental KIEs slightly smaller for the (R)-(+)-enantiomer than for the (S)-(–)-enantiomer indicate that a step preceding the dehalogenation is partly rate-limiting. A small commitment of  $\sim 0.3$  indicates that free energies of activation for the decomposition of the ES complex in the forward and reverse direction are within 1 kcal/mol. The exact nature of this preceding step (or steps) will probably remain unknown until the three-dimensional structure of the DL-DEX 113 becomes available. The isotopic fractionation pattern indicates, however, that it should be characterized by sizable isotope effects with the one in the dissociation direction being substantially larger, leading to the overall inverse deuterium isotope effect under the  $V_{\text{max}}/K_M$  conditions.

In the case of the (S)-(–)-enantiomer, a step after dehalogenation is the overall rate-determining step, while in the case of the (R)-(+)-enantiomer, the dehalogenation is both the first irreversible and overall rate-determining step.

The differences in energetics of the reactions of both enantiomers of 2-chloropropionate catalyzed by the DL-DEX 113 dehalogenase resulting from the conclusions given above are summarized in Figure 3. We conclude that the reaction paths differ in energetic barriers of the steps preceding and following the dehalogenation step; for the (R)-(+)-enantiomer, the preceding barrier is higher and the following barrier is lower than for the (S)-(–)-enantiomer.

## ACKNOWLEDGMENT

We thank Prof. Lesław Gajek for help with the statistical analysis as well as Prof. Daniel M. Quinn and Prof. Richard

L. Schowen for helpful discussion of solvent isotope effects. Access to supercomputer facilities at ICM Warsaw and PCS S Poznan is gratefully acknowledged. This work was supported by grant 4T09A03025 (2003–2006) from the State Committee for Scientific Research, Poland.

## REFERENCES

1. Motosugi, K., Esaki, N., and Soda, K. (1982) Purification and properties of a new enzyme, DL-2-haloacid dehalogenase, from *Pseudomonas* sp., *J. Bacteriol.* **150**, 522–527.
2. Nardi-Dei, V., Kurihara, T., Park, C., Esaki, N., and Soda, K. (1997) Bacterial DL-2-haloacid dehalogenase from *Pseudomonas* sp. strain 113: Gene cloning and structural comparison with D- and L-2-haloacid dehalogenases, *J. Bacteriol.* **179**, 4232–4238.
3. Barth, P. T., Bolton, L., and Thomson, J. C. (1992) Cloning and Partial Sequencing of an Operon Encoding Two *Pseudomonas putida* Haloalkanoate Dehalogenases of Opposite Stereospecificity, *J. Bacteriol.* **174**, 2612–2619.
4. Nardi-Dei, V., Kurihara, T., Park, C., Miyagi, M., Tsunasawa, S., Soda, K., and Esaki, N. (1999) DL-2-Haloacid Dehalogenase from *Pseudomonas* sp. 113 Is a New Class of Dehalogenase Catalyzing Hydrolytic Dehalogenation Not Involving Enzyme–Substrate Ester Intermediate, *J. Biol. Chem.* **274**, 20977–20981.
5. Kurihara, T., Esaki, N., and Soda, K. (2000) Bacterial 2-Haloacid Dehalogenases: Structures and Reaction Mechanisms, *J. Mol. Catal. B: Enzym.* **10**, 57–65.
6. Paneth, P. (2003) Chlorine Kinetic Isotope Effects on Enzymatic Dehalogenations, *Acc. Chem. Res.* **36**, 120–126.
7. Paneth, P. (2006) Chlorine Isotope Effects in Biological Systems, in *Isotope Effects in Chemistry and Biology* (Kohen, A., and Limbach, H. H., Eds.) Chapter 35, pp 875–892, CRC Taylor & Francis Group, Baton Rouge, LA.
8. Iwasaki, I., Utsumi, S., Hagino, K., and Ozawa, T. (1956) A new spectrophotometric method for the determination of small amounts of chloride using the mercuric thiocyanate method, *Bull. Chem. Soc. Jpn.* **29**, 860–864. Bergmann, J. G., and Sanik, J., Jr. (1957) Determination of Trace Amounts of Chlorine in Naphtha, *Anal. Chem.* **29**, 241–243.
9. Quinn, Q. M., and Sutton, L. D. (1991) Theoretical Basis and Mechanistic Utility of Solvent Isotope Effects, in *Enzyme Mechanism from Isotope Effects* (Cook, P. F., Ed.) Chapter 3, pp 73–126, CRC Press, Boca Raton, FL.
10. Westaway, K. C., Koerner, T., Fang, Y.-R., Rudziński, J., and Paneth, P. (1998) A New Method of Determining Chlorine Kinetic Isotope Effects, *Anal. Chem.* **70**, 3548–3552.
11. Lynch, B. J., Fast, P. L., Harris, M., and Truhlar, D. G. (2000) Adiabatic Connection for Kinetics, *J. Phys. Chem. A* **104**, 4811–4815.
12. *Jaguar*, version 6.5 (2005) Schrodinger, LLC, New York.
13. Tannor, D. J., Marten, B., Murphy, R., Friesner, R. A., Sitkoff, D., Nicholls, A., Ringnalda, M., Goddard, W. A., III, and Honig, B. (1994) Accurate First Principles Calculation of Molecular Charge Distributions and Solvation Energies from Ab Initio Quantum Mechanics and Continuum Dielectric Theory, *J. Am. Chem. Soc.* **116**, 11875–11882. Marten, B., Kim, K., Cortis, C., Friesner, R. A., Murphy, R. B., Ringnalda, M., Sitkoff, D., and Honig, B. (1996) New Model for Calculation of Solvation Free Energies: Correction of Self-Consistent Reaction Field Continuum Dielectric Theory for Short-Range Hydrogen-Bonding Effects, *J. Phys. Chem.* **100**, 11775–11788.
14. Simonson, T., and Perahia, D. (1995) Dielectric properties of proteins from simulations: Tools and techniques, *Comput. Phys. Commun.* **91**, 291–303.
15. Melander, L., and Saunders, W. H., Jr. (1980) *Reaction Rates of Isotopic Molecules*, Wiley and Sons, New York.
16. Anisimov, V., and Paneth, P. (1999) ISOEFF98. A Program for Studies of Isotope Effects Using Hessian Modifications, *J. Math. Chem.* **26**, 75–86.
17. Wigner, E. (1932) Über das Überschreiten von Potentialschwellen bei chemischen Reaktionen, *Z. Phys. Chem. B* **19**, 203–216.
18. Meyer, M. P., DelMonte, A. J., and Singleton, D. A. (1999) Reinvestigation of the Isotope Effects for the Claisen and Aromatic Claisen Rearrangements: The Nature of the Claisen Transition States, *J. Am. Chem. Soc.* **121**, 10865–10874.
19. Koch, H. F., McLennan, D. J., Koch, J. G., Tumas, W., Dobsen, B., and Koch, N. H. (1983) Use of Kinetic Isotope Effects in Mechanistic Studies. 4. Chlorine Isotope effects Associated with Alkoxide-Promoted Dehydrochlorination Reactions, *J. Am. Chem. Soc.* **105**, 1930–1937.
20. Lewandowicz, A., Sicińska, D., Rudziński, J., Ichiyama, S., Kurihara, T., Esaki, N., and Paneth, P. (2001) Chlorine Kinetic Isotope Effect on the Fluoroacetate Dehalogenase Reaction, *J. Am. Chem. Soc.* **123**, 9192–9193.
21. Northrop, D. B. (1977) Determining the Absolute Magnitude of Hydrogen Isotope Effects, in *Isotope Effects on Enzyme-Catalyzed Reactions* (Cleland, W. W., O'Leary, M. H., and Northrop, D. B., Eds.) pp 122–152, University Park Press, Baltimore. Cleland, W. W. (1982) Use of isotope effects to elucidate enzyme mechanisms, *CRC Crit. Rev. Biochem.* **13**, 385–428.
22. Lewandowicz, A., Rudziński, J., Tronstad, L., Widersten, M., Ryberg, P., Matsson, O., and Paneth, P. (2001) Experimental and Theoretical Chlorine Kinetic Isotope Effect in the Haloalkane Dehalogenase Reaction, *J. Am. Chem. Soc.* **123**, 4550–4555.
23. Adediran, S. A., Deraniyagala, S. A., Xu, Y., and Pratt, R. F. (1996)  $\beta$ -Secondary and Solvent Deuterium Kinetic Isotope Effects on  $\beta$ -Lactamase Catalysis, *Biochemistry* **35**, 3604–3613.
24. Stein, R. L., and Trainor, D. A. (1986) Mechanism of inactivation of human leukocyte elastase by a chloromethyl ketone: Kinetic and solvent isotope effect studies, *Biochemistry* **25**, 5414–5419.
25. Fang, Y.-R., Gao, Y., Ryberg, P., Eriksson, J., Kołodziejska-Huben, M., Dybała-Defratyka, A., Paneth, P., Matsson, O., and Westaway, K. C. (2003) Experimental and Theoretical Multiple Kinetic Isotope Effects for an SN2 Reaction. An Attempt to Determine Transition State Structure and the Ability of Theoretical Methods to Predict Experimental Kinetic Isotope Effects, *Chem.—Eur. J.* **9**, 2696–2709.
26. Sicińska, D., Rostkowski, M., and Paneth, P. (2005) Chlorine Isotope Effects in Organic Chemistry: Recent Advances, *Curr. Org. Chem.* **9**, 75–88.

B10519553